

# Event Reconstruction for a DIRC

V. Kyryanchuk <sup>a 1</sup>, H. Machner <sup>a,b 2</sup>, R. Siudak <sup>a3</sup>, J. Ritman <sup>a</sup>

<sup>a</sup>Institut für Kernphysik and Jülich Centre for Hadron Physics,  
Forschungszentrum Jülich, 52425 Jülich, Germany

<sup>b</sup>Fachbereich Physik, University Duisburg-Essen, Lotharstr. 1,  
47048 Duisburg, Germany

## Abstract

Monte Carlo simulations were performed to investigate the possibility to add a DIRC detector to the WASA detector at the COSY accelerator. A statistical method for pattern recognition is presented and the possible angle resolution and velocity precision achieved are discussed.

## 1 Introduction

It is planned to measure rare decays of  $\eta'$  mesons with the WASA at COSY detector [1], [2]. The foreseen production reaction is

$$p + p \rightarrow \eta' + p + p \quad (1)$$

where the two protons will be measured and the  $\eta'$  will be identified via missing mass technique. The cross section for this process is small, because no nucleon resonance couples strongly to the  $\eta'p$  channel, in contrary to  $\eta$  production. The  $\eta'$  peak will be on top of a huge multi-pion background. The only chance to identify the  $\eta'$  is to measure the four momentum vectors of the two protons with high accuracy. Although their emission angles  $(\theta, \phi)$  are measured with sufficient precision, their kinetic energies are poorly determined by the present setup. A possible option to achieve sufficient resolutions seems to be a DIRC detector (Detection [of] Internally Reflected Cherenkov [light]) [3] in the forward detection system of WASA. Cherenkov detectors are widely used in high energy physics. They can have different applications: particle identification, energy measuring, threshold detector for detecting specific type of particles in a definite energy range.

Our aim is to measure the velocity of protons in the kinetic energy range from  $T = 400$  MeV to  $T = 1000$  MeV with a precision better than  $\Delta\beta/\beta = 0.5\%$

## 2 DIRC Design

With the Monte Carlo package GEANT3 [4] different radiator materials were studied: LiF, CaF<sub>2</sub>, quartz (fused silica) and plexiglas. All materials have different refractive indices which are smooth functions of the wavelength in the visible range (see Fig. 1). Quartz has the largest values for the refraction index  $n$  at any given wavelength  $\lambda$  compared to the two other materials.  $n$  varies from 1.60 in the UV range to 1.45 in the IR range. The transmittances are rather independent from the wavelength above a certain “threshold” wavelength as is shown in Fig. 2 (data taken from Ref. [5] and [6]). The radiator should have a large refractive index and high transmittance to measure particles with “low” kinetic energy. LiF has higher transmittance in the UV range compared to CaF<sub>2</sub> and quartz. This gives the possibility to build a Cherenkov detector with LiF as radiator and a proper photocathode for detecting photons in the UV range. However, in the visible range, where the transmittance of LiF and quartz are compatible, quartz has the larger refractive index. We therefore omit CaF<sub>2</sub> and LiF in the further studies.

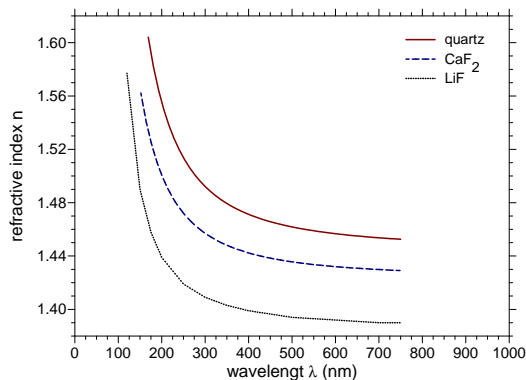


Figure 1: The refractive index  $n$  as function of the wavelength for the indicated materials (from Refs. [5, 6]).

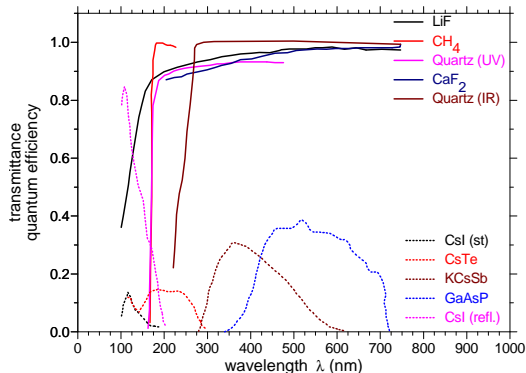


Figure 2: Radiator transmittances (solid curves) [5] and quantum efficiencies of photocathodes (dotted curves) [7–10] as function of the wave length. The bulk transmittances are given for 10 mm thickness and reflection losses at the surface result in an additional reduction of the transmittance by 10%.

The quantum efficiencies for different photocathodes are also shown in Fig. 2 (from Refs. [7–10]). CsI and CsTe are used for photon detecting in the UV range. Bi-alkali (KCsSb) and multi-alkali (GaAsP) photocathodes are used for the near UV and the visible light range. These types of photocathodes have larger and broader distributions of the corresponding quantum efficiency function. This could compensate a lower number of emitted photons in this range of wavelengths. In a first step, simulations were performed for a RICH type Cherenkov detector with different radiators and photon detectors. However, a DIRC type detector was found to be favorable due to following reasons: energy losses in the detector, the broad range of velocities to be measured in the proximity to the Cherenkov threshold and the availability of very fast photon detectors. Based on the above discussed properties of the materials we limit ourselves in the simulations of DIRC detectors to fused silica and UV transparent plexiglas as radiator and photomultipliers with bi-alkali photocathodes.

We will now concentrate on the DIRC detector. The design differs from the Babar DIRC [3, 11]. It consists of radiator bars with dimensions  $2 \times 6 \times 50$   $\text{cm}^3$  and a focusing element with a cylindrical mirror (Figs. 3 and 4). The dimensions were for fused silica whereas for plexiglas an increased thickness of 4 cm was assumed. The individual modules are arranged in two planes, one above and one below the beam axis. The normal axis to each plane is

tilted by  $20^\circ$  away from the beam axis (see Fig. 3). Emitted Cherenkov photons create an image on a pixelised screen. Each pixel is a bi-alkali photocathode with dimension  $5 \times 5 \text{ mm}^2$ .

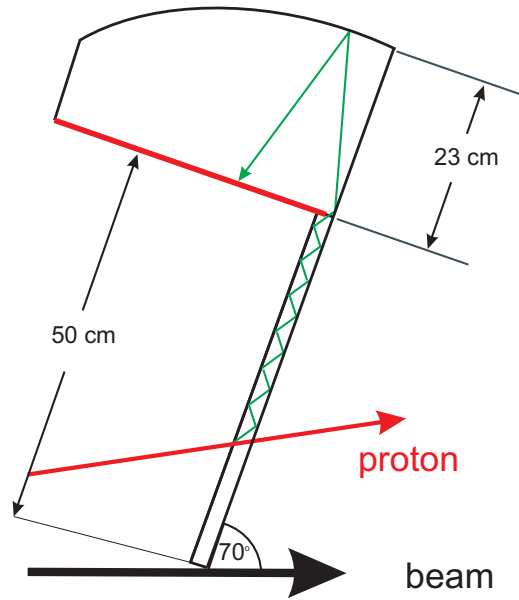


Figure 3: Schematic side view of the detector. The radiator bars are inclined by 70 degree with respect to the beam axis. A simulated proton is indicated with an arrow, the Cherenkov light as the zigzag and arrow. The focussing bar (mirror) is on top.

### 3 Monte Carlo Results

A single event image consists of two arcs, which are the results of the internal reflection from the left and right side of the radiator bar. The shape of the arcs depend on the kinetic energy and particle species. The relative positions of the arcs depend on the horizontal angle of the detected particle track: the larger the horizontal angle, the larger the distance between arc centers [3].

We have simulated Cherenkov images for protons with 600 MeV and 1000 MeV kinetic energy. We applied a left handed coordinate system with the

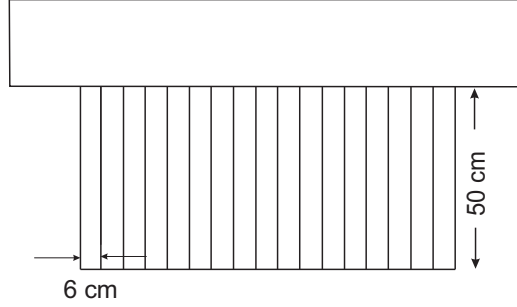


Figure 4: Assembly of several bars to one module. Two such modules are foreseen, one above and one below the beam.

$z$ -axis in the beam direction,  $x - z$  defines the horizontal plane and  $y$  is vertical to this plane. The angle between the ejectile momentum and the  $(x-z)$  plane is  $\theta_{\text{vert}}$  and the angle between the momentum projected in the plane and the beam direction is  $\theta_{\text{horiz}}$ . Thus  $\theta_{\text{horiz}} = \arctan(z_x/p_z)$  and  $\theta_{\text{vert}} = \arcsin(p_y/p)$ . Simulations were performed for track directions  $\theta_{\text{horiz}} \sim 8.5^\circ$  fixed and  $\theta_{\text{vert}}$  varied and vice versa:  $\theta_{\text{vert}} \sim 8.5^\circ$  fixed and  $\theta_{\text{horiz}}$  varied. They are shown in Fig. 5.

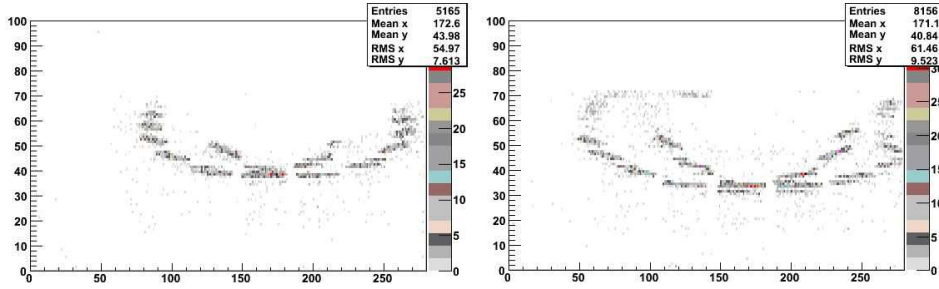


Figure 5: Left: Scatter plot of the position of detected photons from 100 simulated events for protons with kinetic energy  $T= 600$  MeV. The abscissa and ordinate are the horizontal and vertical position numbers on the photocathode. Right: Same as left but for  $T=1000$  MeV

The average number of emitted photons depends on the path through the radiator end the kinetic energy. Fig. 6 shows the dependence of the number of detected photons on the horizontal track direction for protons with

kinetic energy  $T = 600$  MeV. The number of detected photons drops sharply when the particle passes through the edges of the radiator bars. This effect results from the detector construction.

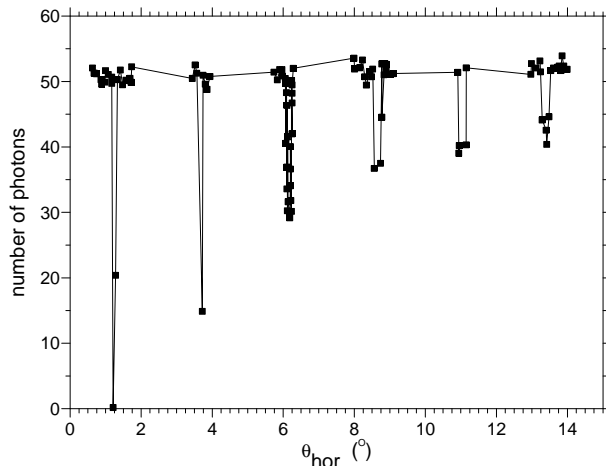


Figure 6: The average number of the detected photons as function of the horizontal angle for protons with  $T = 600$  MeV.

Furthermore, image distortion is also observed. Smearred arcs or even four arcs could be observed when the particle goes through the edges of two neighboring bars.

## 4 Event Reconstruction

The following method is used for event reconstruction. A collection of events with different particle species as well as energies and directions is simulated. Then a second set of simulated data named detected are “compared” to the simulated data. The comparison is realized by the following function  $F$  (2)

$$F(k, (E, P)) = \sum_{i,j} det(i, j) \cdot \overline{sim(i, j)}. \quad (2)$$

Here  $k$  denotes the particle species,  $E, P$  the energy and momentum of the particle,  $det(i, j)$  is the number of detected photons in  $(i, j)$ -th

photoelement in the experiment and  $\overline{sim(i,j)}$  the simulated average number of detected photons in  $(i,j)$ -th photoelement. The expression is a maximum when the experimental image on the screen is similar to the simulated one. This method provides an opportunity to determine  $\beta$  and the direction of a particle if the particle type is known. The particle species information has to come from other sources.

The possibility of track reconstruction for protons with  $T=600$  MeV is demonstrated in Figs. 7 and 8. The particle direction is extracted under the assumption that the particle species and its energy are known.

Horizontal and vertical angles relative to the beam direction are reconstructed given that one of both is fixed. The small widths ( $\sigma$ ) of Gaussians fitted to the data of  $\sim 0.3^\circ$  and  $\sim 0.5^\circ$  indicate the sensitivity of the method. Similar results were obtained for protons with  $T=1000$  MeV.

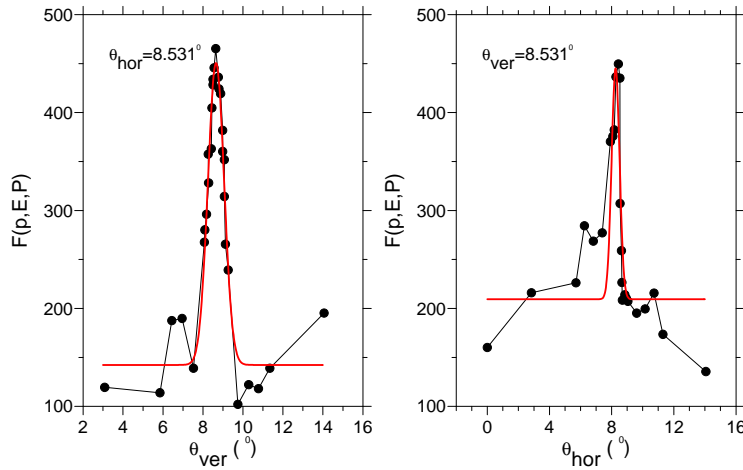


Figure 7: Track reconstruction. Left:  $F$  as function of the vertical angle and for fixed horizontal angle. The results (dots) are connected by lines to guide the eye. The smooth curve is a fit with a Gaussian plus a constant. Right: Same as left but horizontal and vertical angles are interchanged.

Fig. 8 shows the  $\beta$ -resolution for protons. Here we have assumed that the angle measurement is performed with other detectors. The method gives a resolution ( $\sigma_{\beta}/\beta$ ) for protons better than 0.3%. The results obtained can be transformed into the missing mass resolution. For an incident proton beam with 3.3 GeV/c momentum a missing mass resolution of  $\sigma_{mm} \approx 0.5$

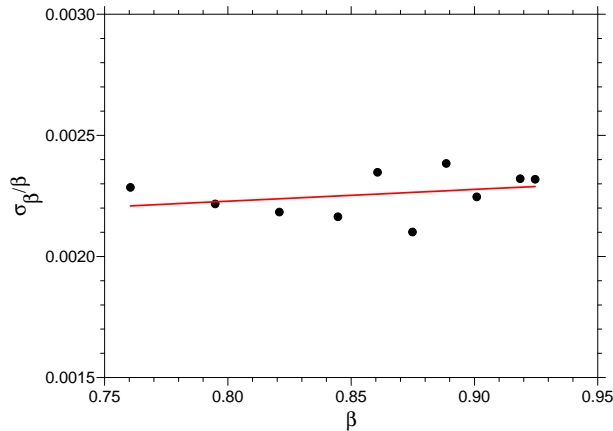


Figure 8: Relative  $\beta$ -resolution for protons as function of  $\beta$ . The results are shown by dots, the solid line is a linear fit to the dots.

MeV is achieved.

## 5 Summary

We have designed a DIRC detector to measure protons with kinetic energy from 400 to 1000 MeV. Monte Carlo simulations for such a device have been performed. A method is discussed to deduce four momentum vectors of the protons. The method gives reliable information for the event reconstruction: velocity-resolution for protons is better than 0.3%. The routine is able to reconstruct tracks and identify particles when additional information is provided by complementary detectors. The large data base of simulated events is a disadvantage of this method; however, optimization of the algorithm will increase the speed.

## References

- [1] WASA-at-COSY Collaboration, H.H. Adam, et al., arXiv:nucl-ex/0411038 (2004).
- [2] WASA-at-COSY Collaboration, C. Adolph, et al., Phys. Lett. **B 677**, 24 (2009).



- [3] P. Coyle et al., Nucl. Instr. and Meth. in Phys. Research **A 343**, 292 (1994).
- [4] R. Brun, F. Bruyant, M. Maire, A.C. McPherson, P. Zancarini, Program package GEANT3, cernlib@cern.ch (1987).
- [5] SCHOTT optical glass data sheets, [www.schott.com](http://www.schott.com).
- [6] Korth Kristalle, [www.korth.de/de/503728952d091450d/index.htm](http://www.korth.de/de/503728952d091450d/index.htm)
- [7] G. R. Carruthers, Applied Optics **8**, 633 (1969).
- [8] A. Breskin, Nucl. Instr. and Methods in Phys. Research **A 371**, 116 (1996).
- [9] K. Kaufmann, <http://www.photonics.com/Content/ReadArticle.aspx?ArticleID=25145>.
- [10] A. Braem, C. Joram, F. Piuz, E. Schyns, J. Séguinot, Nucl. Instr. and Meth. in Phys. Research **A 502**, 205 (2003).
- [11] J. Cohen-Tanugi, M. Convery, B. Ratcliff, X. Sarazin, J. Schwiening, J. Va'vra, Nucl. Instr. and Meth. in Phys. Research **A 515** 680 (2003). 292-299.